Draft version May 8, 2013
Preprint typeset using LaTeX style emulateapj v. 11/10/09

ON THE MINIMUM CORE MASS FOR GIANT PLANET FORMATION THROUGH KELVIN-HELMHOLTZ CONTRACTION

Ana-Maria A. Piso
Harvard-Smithsonian Center for Astrophysics

Andrew N. Youdin
JILA, University of Colorado at Boulder
Draft version May 8, 2013

ABSTRACT

The core accretion model proposes that giant planets form by the accretion of gas onto a solid protoplanetary core. Previous studies have found that there exists a "critical core mass" past which hydrostatic solutions can no longer be found and unstable atmosphere collapse occurs. In standard calculations of the critical core mass, planetesimal accretion deposits enough heat to alter the luminosity of the atmosphere, increasing the core mass required for the atmosphere to collapse. In this study we consider the extreme case in which planetesimal accretion is negligible and Kelvin-Helmholtz contraction dominates the luminosity evolution of the planet. We develop a two-layer atmosphere model with an inner convective region and an outer radiative zone that matches onto the protoplanetary disk, and we determine the minimum core mass for a giant planet to form within the typical disk life timescale for a variety of disk conditions, which we denote as "critical core mass". We find that the absolute minimum core mass required to nucleate atmosphere collapse within the disk lifetime is smaller for planets forming further away from their host stars. Moreover, the critical core mass is strongly dependent on disk temperature, opacity and mean molecular weight of the gas. Our results yield lower mass cores than corresponding studies for large planetesimal accretion rates. We therefore show that it is easier to form a planet by growing the core first, then accreting a massive gaseous envelope, rather than forming the core and atmosphere simultaneously.

1. INTRODUCTION **(PAPER II)**

Current theories of giant planet formation postulate that these planets form either through core accretion (refs), in which solid planetesimals collide and grow into a massive solid core, which then accretes a gaseous envelope, or due to a gravitational instability in the protoplanetary disk that leads to fragmentation of the disk into self-gravitating clumps (refs, inc. D'Angelo et al. 2011).

Standard core accretion models (refs) assume that the core and the atmosphere grow at the same time, and that planetesimal accretion deposits enough heat to alter the luminosity of the atmosphere, increasing the core mass required for the atmosphere to collapse, while the heat generated by the gravitational (Kelvin-Helmholtz) contraction of the atmosphere is neglected. These studies consider that the planet atmosphere is in steady state, in which all the luminosity due to planetesimal accretion is radiated away by the envelope, and find that there exists a minimum ("critical") core mass past which hydrostatic solutions can no longer be found and unstable atmosphere collapse occurs.

Forming giant planets at wide separations in the disk poses theoretical challenges. On the one hand, gravitational instability generates objects that are too massive to explain the current observed properties of exoplanets (refs, inc. Rafikov 2005). On the other hand, planetesimal accretion is slow at large distances in the disk, and therefore large cores may not be able to form before the dissipation of the disk (refs). I would therefore be easier if giant planets could form from smaller cores which would need less time to grow.

In this study, we show that giant planets can grow faster from small protoplanetary cores that are fully formed before significant gas accretion occurs. In this scenario, the planetesimal accretion rate is significantly slowed down during the gas contraction phase of the atmosphere. This reduction can arise due to dynamical clearing, or due to the core having formed in the inner parts of the disk and migrated outwards, etc. In this situation, the atmosphere evolution is dominated by the Kelvin-Helmholtz contraction of the envelope. The atmosphere is no longer in a steady state, but rather it accretes gas as it loses energy through radiation.

In our model we therefore assume that the luminosity evolution of the atmosphere is dominated by gas contraction, while the planetesimal accretion rate is negligible. As a result, the protoplanetary core has a fixed mass. We consider that the atmosphere evolves in time through stages of quasi-static equilibrium. Once the mass of the gaseous envelope becomes comparable to the mass of the solid core, the self-gravity of the atmosphere can no longer balance the pressure gradient and unstable hydrodynamic collapse commences. The time required for the atmosphere to grow to this stage is the characteristic growth time of the atmosphere. For a set of fixed gas and disk conditions, there exists a minimum core mass for which the atmosphere can grow on the time scale described above within the life time of the protoplanetary disk, which we define as the "critical core mass".

We develop a two-layer atmosphere model, with a convective inner region and a radiative outer region that

matches smoothly on to the protoplanetary disk, and develop a cooling model that evolves the atmosphere in time. We aim to find the critical core mass for a giant planet to form before the dissipation of the disk.

This paper is organized as follows. In section 2 we describe the assumptions of our atmosphere model, and derive the basic equations that govern the structure and evolution of the atmosphere. In section 3, we present a simplified analytic model that predicts the qualitative behavior of the numerical model. We describe our results in section 4, and determined the critical core mass for planet formation during the life time of the protoplanetary disk in section 5. We discuss our results in section 6 and summarize our findings in section 7.

2. ATMOSPHERE MODELS **(PAPER I)**

In this section we derive the structure and evolution of a planetary atmosphere embedded in a protoplanetary disk in the absence of planetesimal accretion. In section 2.1 we describe the assumptions of our model. In section 2.2 we describe the properties of our assumed protoplanetary disk and review relevant length scales. Section 2.3 presents the equations describing the structure of a static planetary atmosphere and the boundary conditions that we use. In section 2.4 we develop a model to estimate the rate at which the atmosphere cools. Finally, we combine these calculations into a quasi-static model for atmospheric evolution in section 2.5.

2.1. *Basic Model Assumptions*

We develop a two-layer atmosphere model with the following assumptions:

1. The planet consists of a solid core of fixed mass and a two-layer atmosphere composed of an inner convective zone and an outer radiative zone that matches smoothly on to the disk, as mentioned in section. The two regions are separated by the Schwarzschild criterion for convective instability (see section 2.3). We denote the surface between the two regions as the radiative-convective boundary (RCB), which is henceforth defined by a radius $r = R_{RCB}$.

2. The luminosity evolution of the atmosphere is dominated by Kelvin-Helmholtz contraction rather than planetesimal accretion.

3. The luminosity is assumed to be constant throughout the outer radiative region. Since the structure of the convective zone is independent of its luminosity, we do not need to make additional assumptions about the luminosity in this region.

4. The envelope evolves through stages of quasi-static equilibrium.

We use assumptions for the atmosphere geometry and composition similar to those of previous studies (e.g., Ikoma et al. 2000, Papaloizou & Nelson 2005), as follows:

1. The atmosphere is self-gravitating, spherically symmetric and in hydrostatic balance.

2. The atmosphere consists of a hydrogen-helium mixture, with hydrogen and helium mass fractions of 0.7 and 0.3, respectively.

The time dependence of the atmosphere structure equations may be neglected or explicitly taken into account. Some previous studies of atmosphere accretion (e.g., Stevenson 1982, Wuchterl 1993, Rafikov 2006) consider static envelopes, in which the luminosity is solely supplied by planetesimal accretion and fully radiated away by the atmosphere. In other studies, the time evolution is explicitly taken into account and full time dependent models are developed (e.g., Ikoma et al. 2000). We follow an intermediate approach and consider quasi-static evolution. Our model for the atmosphere growth time is described in section 2.4.

2.2. *Disk Model and Length Scales*

As a disk model, we use the minimum mass, passively irradiated model of Chiang & Youdin (2010). In this model, the surface density and mid-plane temperature are given by

$$\Sigma_d = 2200 F_\Sigma a^{-3/2} \text{ g cm}^{-2} \quad (1a)$$

$$T_d = 120 F_T a^{-3/7} \, K, \quad (1b)$$

with a the semi-major axis in AU, and F_Σ and F_T normalization factors that adjust the disk mass and temperature relative to the minimum mass solar nebula (MMSN). In this study, we assume $F_\Sigma = F_T = 1$. The resulting mid-plane pressure is given by

$$P_d = 1.1 \times 10^{-4} F_\Sigma \sqrt{F_T m_*} a^{-45/14} \text{ dyne cm}^{-2} \quad (2)$$

for a molecular weight $\mu = 2.35$. Here $m_* \equiv M_*/M_\odot$, where M_* is the mass of the central star and $M_\odot$ is the mass of the Sun. We take $m_* = 1$.

We further define several characteristic length scales that are important for this problem.

The Core Radius represents the physical radius of the protoplanetary core:

$$R_c \equiv \left(\frac{3M_c}{4\pi\rho_c}\right)^{1/3}, \quad (3)$$

with M_c and ρ_c the core mass and density, respectively. Since we assume that the core mass does not change with time, the core radius is also fixed for a given model.

The Bondi Radius represents the distance from the planet at which the thermal energy of the nebular gas is of the order of the gravitational energy binding the gas to the planet. It is defined as

$$R_B \equiv \frac{GM_p}{c_s^2} = \frac{GM_p}{\mathcal{R}T_d}, \quad (4)$$

where G is the gravitational constant, M_p is the total mass of the planet, c_s is the sound speed, and $\mathcal{R}$ is the reduced gas constant: $\mathcal{R} = k_b/(\mu m_p)$, with k_b the Boltzmann constant and m_p the proton mass.

The Hill Radius represents the distance at which the gravitational attraction of the planet and of the host star are comparable. It is given by

$$R_H \equiv a\Big(\frac{M_p}{M_\odot}\Big)^{1/3} \tag{5}$$

Outside the Hill radius, the gravity of the core is too weak to affect the nebular gas. Consequently, the planet will be able to accrete only gas that lies within its Hill sphere.

The Disk Scale Height is defined by

$$H \equiv \frac{c_s^2}{\Omega}, \tag{6}$$

where Ω is the Keplerian angular velocity. The disk scale height is a measure of the thickness of the protoplanetary disk. Using equation (1a), we find that the scale height for our assumed disk model can be expressed as

$$H = 0.022\sqrt{F_T}a^{9/7}\ \text{AU} \tag{7}$$

For small planet masses, $R_B < R_H < H$. As the atmosphere becomes more massive, tidal truncation becomes more important than thermal constraints, and $R_H < R_B < H$. Finally, for high mass atmospheres the disk scale height becomes smaller than the Hill radius of the planet, and spherical symmetry breaks, as the planet is now affected by the vertical profile of the disk.

2.3. *Structure Equations and Boundary Conditions*

An atmosphere in hydrostatic equilibrium is fully described by the following structure equations:

$$\frac{dP}{dr} = -\frac{Gm}{r^2}\rho \tag{8a}$$
$$\frac{dm}{dr} = 4\pi r^2\rho \tag{8b}$$
$$\frac{dT}{dr} = \nabla\frac{T}{P}\frac{dP}{dr} \tag{8c}$$
$$\frac{dL}{dr} = 4\pi r^2\rho\epsilon_g, \tag{8d}$$

where r is the radial coordinate, P, T and ρ are the gas pressure, temperature and density, respectively, m is the mass enclosed by the radius r, L is the luminosity from the surface of radius r, and $\epsilon_g \equiv -T\frac{ds}{dt}$ represents the heating per unit mass due to gravitational contraction, with s the specific gas entropy. The temperature gradient $\nabla \equiv \frac{d\ln T}{d\ln P}$ has different expressions depending on the primary means of energy transport throughout the atmosphere. We assume that energy can be transported either through radiation or convection. When the luminosity is carried by radiative diffusion, the temperature gradient is given by

$$\nabla = \nabla_{\rm rad} \equiv \frac{3\kappa P}{64\pi Gm\sigma T^4}L, \tag{9}$$

where σ is the Stefan-Boltzmann constant and κ is the opacity. Alternatively, when the energy is transported outwards through convective motions, the temperature gradient becomes

$$\nabla = \nabla_{\rm ad} \equiv \Big(\frac{d\ln T}{d\ln P}\Big)_{\rm ad}, \tag{10}$$

where $\nabla_{\rm ad}$ is the adiabatic temperature gradient. For an ideal gas of adiabatic index γ, $\nabla_{\rm ad} = \frac{\gamma-1}{\gamma}$. The process that dominates energy transport throughout the atmosphere is determined by the Schwarzschild criterion (e.g., Thompson 2006): the atmosphere is stable against convection when

$$\nabla < \nabla_{\rm ad} \tag{11}$$

and convectively unstable when the reverse is true. In order for convection to be effective, $\nabla \approx \nabla_{\rm ad}$. Therefore, we find that the temperature gradient is given by $\nabla = \min(\nabla_{\rm ad}, \nabla_{\rm rad})$.

In order for equation set (8) to be solvable, it has to be supplemented by an equation of state (EOS) that relates pressure, temperature and density $P = P(\rho, T)$, and an opacity law for κ. In our study, we assume an ideal gas polytropic EOS

$$P = K\rho^\gamma = K\rho^{1/(1-\nabla_{\rm ad})}, \tag{12}$$

with K the adiabatic constant. The adiabatic gradient is $\nabla_{\rm ad} = 2/5$ for a monatomic gas and $\nabla_{\rm ad} = 2/7$ for a diatomic gas. Additionally, the ideal gas law relates the pressure, temperature and density through

$$P = \rho\mathcal{R}T, \tag{13}$$

with $\mathcal{R}$ defined in section 2.1. The specific gas constant $\mathcal{R}$ depends on the mean molecular weight of the gas μ. μ is determined by the relative abundance of hydrogen and helium in the atmosphere. In this study we assume that the helium fraction only affects the molecular weight of the gas, and not the adiabatic index. We show in section 5.4 that this assumption does not affect the qualitative behavior of our solutions.

We assume an opacity power law of the form

$$\kappa = \kappa_0\Big(\frac{P}{P_d}\Big)^\alpha\Big(\frac{T}{T_d}\Big)^\beta, \tag{14}$$

with α and β constants, and $\kappa_0 = 2F_\kappa$. To estimate α and β we use the Bell & Lin (1994) opacity laws for ice grains: $\alpha = 0$, $\beta = 2$ and $F_\kappa = 1$ (i.e., $\kappa_0 = 2$). We note that these values are valid only for low disk temperatures: $T_d <\sim 100K$. As such, we only consider cool atmospheres that form in the outer part of the protoplanetary disk ($a \geq 10$ AU).

2.3.1. *Boundary Conditions*

We assume a solid core of fixed mass M_c with a radius given by equation (3). We choose $\rho_c = 3.2$ g cm^{-3} (e.g., Papaloizou & Terquem 1999). Furthermore, we assume the atmosphere extends out to the boundary of the Hill sphere, defined by equation (5). If the Bondi radius (defined in equation (4)) is within the Hill radius, perturbations of the nebular gas still occur past the Bondi radius due to the gravitational influence of the core. If,

on the other hand, $R_B > R_H$, then the Hill radius is the more relevant truncation radius since material cannot be gravitationally bound to the protoplanet outside the Hill sphere. As such, it is always safe to choose the Hill radius as the outer boundary.

As stated in section 2.1, the atmosphere matches smoothly onto the disk at the outer boundary. The temperature and pressure at the Hill radius have to therefore be given by the nebular temperature and pressure: $T(R_H) = T_d$ and $P(R_H) = P_d$.

2.4. *Virial Equilibrium and Global Cooling Model*

Section 2.3 provides the structure model for a static atmosphere. We now derive the time evolution of the atmosphere due to Kelvin-Helmholtz contraction between subsequent static models.

We first describe the general ways in which planetary Klevin-Helmholtz contraction differs from the stellar case.

An isolated sphere, such as a star, satisfies a simple global energy equation:

$$L = \Gamma - \dot{E}, \tag{15}$$

where the total luminosity L is balanced by the rate of heat generation Γ (due to nuclear fusion in the case of star) and the rate at which total energy is lost $\dot{E}$. The total energy of the sphere is given by the sum of the gravitational and internal energies.

A protoplanetary atmosphere that is not isolated, but is embedded in a gas disk, satisfies a more complex cooling equation:

$$L = L_c + \Gamma - \dot{E} + e_{\rm acc}\dot{M} - P_M\frac{\partial V_M}{\partial t} \tag{16}$$

This cooling model applies at any radius R where the mass enclosed is M, for example the Bondi radius or the Hill radius. L, Γ and $\dot{E}$ are the same as in equation (15), and include the atmosphere from the core to the top boundary. The gravitational energy E_G of an atmosphere with total mass M is given by

$$E_G = -\int_{M_c}^{M}\frac{Gm}{r}dm, \tag{17}$$

while the internal energy is

$$U = \int_{M_c}^{M} u dm, \tag{18}$$

where u is the internal energy per mass. We now explain the additional terms in the cooling equation (16). L_c is the luminosity from the solid core, and may include planetesimal accretion and radioactive decay. $e_{\rm acc}$ is the specific total energy brought in by mass accreting at the rate $\dot{M}$: $e_{\rm acc} = u - GM/R$. The last term represents the work done on a surface mass element.

The global cooling equation can be derived starting from the local cooling balance. Integrating the local energy equation and (8d) from the core to the surface and using equation (8b) yields

$$\begin{aligned} L - L_c &= \int_{M_c}^{M}\frac{\partial L}{\partial m}dm && \text{(19a)}\\ &= \int_{M_c}^{M}\Big(\epsilon - T\frac{\partial s}{\partial t}\Big)dm && \text{(19b)}\\ &= \Gamma - \int_{M_c}^{M}\frac{\partial u}{\partial t}dm + \int_{M_c}^{M}\frac{P}{\rho^2}\frac{\partial \rho}{\partial t}dm, && \text{(19c)}\end{aligned}$$

where $\Gamma = \int_{M_c}^{M}\epsilon dm$ and equation (19c) follows from equation (19b) through the first law of thermodynamics.

Moreover, a self-gravitating protoplanetary atmosphere has to satisfy virial equilibrium. The virial theorem is derived by integrating the equation of hydrostatic balance (8a) and has the form

$$E_G = -3\int_{M_c}^{M}\frac{P}{\rho}dm + 4\pi(R^3P_M - R_c^3Pc) \tag{20}$$

Similarly to the cooling equation, it applies at any radius R where the total mass enclosed is M. For an ideal gas of adiabatic index γ, equation (20) leads to the following expression for the total energy:

$$\begin{aligned} E &= (1-\xi)U + 4\pi(R^3P_M - R_c^3Pc) && \text{(21a)}\\ &= \frac{\xi-1}{\xi}E_G + \frac{4\pi}{\xi}(R^3P_M - R_c^3Pc) && \text{(21b)}\end{aligned}$$

The global cooling equation (16) can therefore be derived using equations(19) and (20). A detailed derivation is deferred to Appendix A.

2.5. *Quasi-Static Two-Layer Model*

As a consequence of the equations derived in section 2.4, both the atmosphere structure and the gas accretion rate are uniquely determined by the current atmosphere mass. As this mass accretion rate is slow compared to the time it takes to relax to this solution, we can make a quasi-static model of the atmosphere growth. In this section we therefore describe the procedure to obtain an evolutionary series from the cooling model introduced in 2.4 between consecutive two-layer static atmospheres (cf. 2.1).

We use the boundary conditions and opacity laws described in section 2.3. The numerical integration is performed through the shooting method, which solves the boundary value problem by reducing it to an initial value problem: trial values are chosen for the parameters at one of the boundaries, then the equations are integrated and the resulting values at the other boundary are compared to the actual boundary conditions. The procedure is repeated until convergence is achieved. We start with a total atmosphere mass M_i, where the index i labels each evolutionary stage. For this mass we guess a trial luminosity $L = L_{\rm guess}$. The assumption of constant luminosity throughout the radiative zone sets the right hand side of equation (8b) to zero, i.e. the time dependence is neglected. We integrate the structure equations (8) inwards from $R_{\rm out} = R_H$, with the boundary conditions

$T(R_{\rm out}) = T_d$ and $P(R_{\rm out}) = P_d$. The numerical integration gives a value for the core mass implied by the trial solution $M_c = M_{c,\rm guess}$. We adjust $L_{\rm guess}$ until $M_{c,\rm guess}$ converges to the actual core mass M_c.

The time evolution of the atmosphere is obtained using the global cooling model described in section 2.4. We neglect the luminosity due to planetesimal accretion and direct heat generation; as such, the first two terms in equation (16) are set to zero. Equation (16) is then evaluated at the RCB, since we assume that luminosity is primarily generated in the convective zone. In what follows, X_{RCB} denotes quantity X evaluated at the RCB. The time step Δt_i between two consecutive models of masses M_i and M_{i+1} is calculated as follows:

$$< L >_i \Delta t_i = -\Delta E_{RCB,i} + < e_{{\rm acc},RCB} >_i \Delta M_{RCB,i} - < P_{RCB} >_i \Delta V_{RCB,M,i} \quad (22)$$

where we denote

$$\Delta X_i = X_{i+1} - X_i \quad (23a)$$

$$< X >_i = \frac{X_i + X_{i+1}}{2} \quad (23b)$$

The subscript M in the volume expression above signifies evaluating the change in volume at constant mass.

By connecting sets of subsequent static atmospheres through the procedure described above we therefore obtain an evolutionary atmosphere series.

3. ANALYTIC COOLING MODEL **(PAPER I)**

In this section we derive a simplified analytic model for the atmosphere structure and evolution, based on the assumptions and equations described in section 2. We use this model to predict the qualitative behavior of our more detailed numerical model.

We consider a two-layer atmosphere structure model as presented in section 2.1. We approximate the outer radiative zone of the atmosphere as nearly isothermal. Moreover, we do not take into account the self-gravity of the atmosphere in either region. In the next subsections we derive the structure and cooling behavior of such an atmosphere, deferring some of the calculations to Appendix B.

3.1. *Isothermal Atmosphere*

We now consider the structure of a low mass (non self-gravitating) isothermal atmosphere. We assume the atmosphere matches onto a constant background density, $\rho_{\rm o}$, at a distance $r_{\rm fit} = n_{\rm fit} R_{\rm B}$. The resulting density profile is

$$\rho = \rho_{\rm d} \exp\left(\frac{R_B}{r} - \frac{1}{n_B}\right) \approx \rho_{\rm d} \exp\left(\frac{R_B}{r}\right), \quad (24)$$

where the approximate inequality holds deep inside the atmosphere ($r \ll R_{\rm B}$) for any $n_{\rm fit} \gtrsim 1$. However the choice of boundary condition does have an order unity effect on the density near the Bondi radius. In our study, $n_{\rm fit} = R_{\rm B}/R_{\rm H}$, when the Bondi radius is larger than the Hill radius, and $n_{\rm fit} = 1$ when the opposite is true.

The mass of the atmosphere is typically determined by integrating the density profile from the core to the Bondi radius. Planets can attract massive atmospheres if $\theta_{\rm c} \equiv R_B/R_{\rm c} \gg 1$. In this case

$$M_{\rm iso} \approx 4\pi\rho_{\rm o} \frac{R_{\rm c}^4}{R_B} e^{R_B/R_{\rm c}} = 4\pi\rho_{\rm o} \frac{R_{\rm c}^3}{\theta_{\rm c}} e^{\theta_{\rm c}}. \quad (25)$$

This result is the leading order term in a series expansion. Furthermore, because the atmospheric scale-height at $R_{\rm c}$ is $H_\rho = |dr/d\ln\rho| = R_{\rm c}^2/R_B$, the result is intuitively the correct order of magnitude.

3.2. *Temperature and Pressure Corrections at the Radiative-Convective Boundary*

We now show that the temperature contrast between the radiative-convective boundary $T_{\rm RCB}$ and the ambient disk $T_{\rm d}$, is modest. From equation (9), we express the radiative lapse rate

$$\nabla_{\rm rad} = \frac{3\kappa P}{64\pi G M \sigma T^4} L = \nabla_{\rm o} \frac{(P/P_{\rm d})^{1+\alpha}}{(T/T_{\rm d})^{4-\beta}} \quad (26)$$

where the second equality follows from the opacity law (14), and $\nabla_{\rm o}$ is the radiative temperature gradient at the disk:

$$\nabla_{\rm o} \equiv \frac{3\kappa_0 P_{\rm d}}{64\pi G M \sigma T_{\rm d}^4}. \quad (27)$$

M is the sum of the core mass and the atmosphere mass below the pressure level P. If the mass in the radiative zone is small, then we can hold M fixed at the sum of the core and convective zone masses: $M = M_{\rm c} + M_{\rm conv}$. With this assumption and power-law opacity, we get a constant value for $\nabla_{\rm o}$. The temperature profile then integrates to

$$\left(\frac{T}{T_{\rm d}}\right)^{4-\beta} - 1 = \frac{\nabla_{\rm o}}{\nabla_\infty}\left[\left(\frac{P}{P_{\rm d}}\right)^{1-\alpha} - 1\right], \quad (28)$$

where $\nabla_\infty = (1+\alpha)/(4-\beta)$ is $\nabla_{\rm rad}$ for $T, P \to \infty$.[1] We apply Equations (26) and (28) at the radiative-convective boundary (where $\nabla_{\rm rad} = \nabla_{\rm ad}$) under the assumption that the pressure there is $P_{\rm RCB} \gg P_{\rm d}$, motivated by the fact that the exponential density and hence pressure profile is isothermal (see equation (24)). The resulting temperature contrast at the radiative-convective boundary is

$$\chi \equiv \frac{T_{\rm RCB}}{T_{\rm d}} \simeq \left(1 - \frac{\nabla_{\rm ad}}{\nabla_\infty}\right)^{-\frac{1}{4-\beta}}. \quad (29)$$

For $\alpha = 0$ and $\beta = 2$, and assuming $\nabla_{\rm ad} = 2/7$, we find $\chi \approx 1.5$. Values of χ and ∇_∞ for other choices of β are summarized in Appendix B.

The pressure at the convective boundary follows from Equations (9) and (29) as

$$\frac{P_{\rm RCB}}{P_{\rm d}} \simeq \left(\frac{\nabla_{\rm ad}/\nabla_{\rm o}}{1 - \nabla_{\rm ad}/\nabla_\infty}\right)^{\frac{1}{1+\alpha}} \quad (30)$$

This pressure contrast can be quite large due to the smallness of $\nabla_{\rm o}$ in low luminosity atmospheres.

[1] Our definitions of $\nabla_{\rm o}$ and ∇_∞ are precisely opposite to Rafikov (2006), but consistent with other works and the general convention of labeling a quantity f in the disk as $f_{\rm o}$.

It is also useful to obtain a relation between T and P that eliminates $\nabla_{\rm o}$ in favor of $P_{\rm RCB}$:

$$\frac{T}{T_{\rm d}} = \left\{ 1 + \frac{1}{\frac{\nabla_\infty}{\nabla_{\rm ad}} - 1} \left[\left(\frac{P}{P_{\rm RCB}} \right)^{1-\alpha} - \left(\frac{P_{\rm d}}{P_{\rm RCB}} \right)^{1-\alpha} \right] \right\}^{\frac{1}{4-\beta}} . \tag{31}$$

We can determine the radius of the convective boundary $R_{\rm RCB}$ from the hydrostatic balance equation as

$$\frac{R_B}{R_{\rm RCB}} = \int_{P_{\rm o}}^{P_{\rm RCB}} \frac{T}{T_{\rm d}} \frac{dP}{P} . \tag{32}$$

An isothermal atmosphere gives a simple logarithmic dependence on $P_{\rm RCB}$. However using Equation (31) in the integral gives

$$\frac{R_B}{r_{\rm RCB}} = \ln \left(\frac{P_{\rm RCB}}{P_{\rm o}} \right) - \ln \theta , \tag{33}$$

with an extra correction term, $\theta < 1$. The form we chose for the correction term allows us to relate the disk and radiative-convective boundary pressures as :

$$P_{\rm RCB} = \theta P_{\rm d} e^{R_B/R_{\rm RCB}} . \tag{34}$$

In the $P_{\rm RCB} \gg P_{\rm d}$ limit the correction term is an order unity constant that depends on α, β and $\nabla_{\rm ad}$. Similarly to the temperature correction factor χ, θ accounts for the fact that the radiative region is not perfectly isothermal. For $\nabla_{\rm ad} = 2/7$, we find $\theta(\alpha = 0, \beta = 20) \approx 0.556$. Values of θ for other choices of β are summarized in Appendix B. A simple analytic expression for θ is not possible.

3.3. *Simplified cooling model*

We now use a simplified version of the cooling model introduced in section 2.4 in order to obtain an analytic cooling model. As before, we assume a polytropic equation of state and neglect self-gravity.

3.3.1. *Luminosity, Energy & Mass*

From equation (26), the luminosity that emerges at the radiative-convective boundary is

$$L_{\rm RCB} = \frac{64\pi G M_{\rm RCB} \sigma T_{\rm RCB}^4}{3\kappa P_{\rm RCB}} \nabla_{\rm ad} \approx L_{\rm o} \frac{P_{\rm d}}{P_{\rm RCB}}, \tag{35}$$

where we drop the pressure dependence from the opacity law (14) and

$$L_{\rm o} \equiv \frac{64\pi G M_{\rm RCB} \sigma T_{\rm d}^4}{3\kappa(T_{\rm d}) P_{\rm d}} \nabla_{\rm ad} \chi^{4-\beta} \tag{36}$$

normalized to disk conditions, with $T = \chi T_{\rm d}$ at the RCB.

For $\beta = 2$ and $F_\kappa = 1$ in the opacity law (14), this gives the Bell & Lin (1994) opacity for icy grains. By varying F_κ, dust depletion or enhancement can be considered. Grain properties affect both F_κ and β which generally satisfies $1/2 \lesssim \beta \lesssim 2$ (aside from discontinuities across sublimation regions, see Semenov et al. (2003)).

To make further analytic progress, we ignore the self-gravity in the convective zone, holding the mass fixed at $M_{\rm c}$. The density profile of an adiabatic atmosphere follows from hydrostatic balance as

$$\rho = \rho_{\rm RCB} \left[1 + \frac{R'_B}{r} - \frac{R'_B}{R_{\rm RCB}} \right]^{1/(\gamma-1)} . \tag{37}$$

where we define an effective Bondi radius,

$$R'_B \equiv \frac{G M_{\rm c}}{C_P T_{\rm RCB}} = \frac{\nabla_{\rm ad}}{\chi} R_B \tag{38}$$

to simplify expressions.

Deep in the atmosphere, where $r \ll R_{\rm RCB} \lesssim R'_B$ the density profile is $\rho \propto r^{-1/(\gamma-1)}$. Since the energy scales as $\rho r^2 \propto r^{(2\gamma-3)/(\gamma-1)}$ only polytropes with $\gamma < 3/2$ (i.e. $\gamma = 7/5$, but not $\gamma = 5/3$) have the bulk of energy at the bottom of the atmospheres. We will thus focus on the $\gamma = 7/5$ case, even though dissociation occurs deep in real protoplanetary atmospheres.

The total (thermal and gravitational) energy in an adiabatic atmosphere could be evaluated from the virial theorem (see section 2.4). More simply, we use the result for temperature profiles in deep (but non-self-gravitating) convective regions:

$$T \approx \frac{G M_{\rm c}}{C_P r} = T_{\rm RCB} \frac{R'_B}{r} . \tag{39}$$

The internal energy per unit mass of an ideal gas is thus $u = C_V T = (1 - \nabla_{\rm ad}) G M_{\rm c}/r$ and the specific energy deep in the atmosphere is

$$e = e_g + u = -\nabla_{\rm ad} \frac{G M_{\rm c}}{r} . \tag{40}$$

Thus the total energy for $\gamma < 3/2$ is thus

$$E = -4\pi \nabla_{\rm ad} G M_{\rm c} \int_{R_{\rm c}}^{r_{\rm RCB}} \rho r dr \tag{41}$$

$$\approx -4\pi P_{\rm RCB} {R'_B}^{\frac{1}{\nabla_{\rm ad}}} \left(\frac{\gamma - 1}{3 - 2\gamma} \right) R_{\rm c}^{\frac{2\gamma-3}{\gamma-1}} \tag{42}$$

$$\approx -8\pi P_{\rm RCB} \frac{{R'_B}^{7/2}}{\sqrt{R_{\rm c}}} \tag{43}$$

where the final expression takes $\gamma = 7/5$.

The mass of the adiabatic atmosphere is given by

$$M_{\rm atm} = 4\pi \int_{R_{\rm c}}^{R_{\rm RCB}} \rho r^2 dr \tag{44}$$

$$= \frac{5\pi^2}{4} \rho_{\rm RCB} {R'_B}^{5/2} \sqrt{R_{\rm RCB}} \tag{45}$$

in the limit $R_{\rm c} \ll R_{\rm RCB} \ll R'_B$. The mass in the isothermal region is $M_{\rm iso} \sim 4\pi \rho_{\rm RCB} r_{\rm RCB}^4 / R_B \ll M_{\rm atm}$, and can be neglected.

We can eliminate $R_{\rm RCB}$ using Equation (34). The ratio of atmosphere to core mass is then

$$\frac{M_{\rm atm}}{M_{\rm c}} \approx \frac{P_{\rm RCB}/P_M}{\sqrt{\ln[P_{\rm RCB}/(\theta P_{\rm d})]}} \tag{46}$$

where we introduce a characteristic pressure

$$P_M \equiv \frac{4 \nabla_{\rm ad}^{3/2}}{5\pi^2 \sqrt{\chi}} \frac{G M_{\rm c}^2}{{R'_B}^4} . \tag{47}$$

For the atmosphere to initiate unstable gas accretion, $M_{\rm atm} = M_{\rm c}$. We thus require

$$P_{\rm RCB} = \xi P_M \tag{48}$$

where the logarithmic factor

$$\xi \equiv \sqrt{\ln[P_{\rm RCB}/(\theta P_{\rm d})]} = \sqrt{\ln[\xi P_M/(\theta P_{\rm d})]} \quad (49)$$

is found by numerically solving the above transcendental equation. The physical solution has $\xi > 1$, but typically order unity. Numerical solutions exist for $\xi \ll 1$, but are unphysical as they imply $P_{\rm RCB} < P_{\rm d}$.

3.3.2. *Cooling Time*

Neglecting the surface terms from equation (16), the total time to cool the atmosphere from an initially fully adiabatic state is [2]

$$t_{\rm cool} = -\int \frac{dE}{L} = -\int_{P_{\rm o}}^{P_{\rm RCB}} \frac{dE/dP_{\rm RCB}}{L} dP_{\rm RCB} \quad (50)$$

$$\approx 4\pi \frac{P_{\rm RCB}^2}{P_{\rm o}} \frac{R_B'^{7/2}}{L_{\rm o}\sqrt{R_{\rm c}}}, \quad (51)$$

where we neglect self-gravity and take $M_{\rm RCB} = M_{\rm c}$ in $L_{\rm o}$.

The cooling timescale for an atmosphere to become self-gravitating is found from Equations (51) and (48) as

$$t_{\rm cool} \approx 2 \times 10^8 \frac{F_T^{5/2} F_\kappa \left(\frac{\xi}{3.4}\right)^2}{\left(\frac{m_{\rm c\oplus}}{10}\right)^{5/3} \left(\frac{a}{10}\right)^{\frac{15}{14}}} \text{ yr} \quad (52)$$

for $\beta = 2$ and $m_{\rm c\oplus} \equiv M_{\rm c}/M_\oplus$. Clearly this timescale is too long, and this is likely due to missing physics of self-gravity and EOS. Nevertheless the trends are informative. A reduction in opacity naturally gives faster cooling, as long as the optically thick assumption holds. Lower disk temperatures also give faster cooling. Even though higher temperatures give higher luminosities, they also give higher dust opacities and lower the Bondi radius and gas density. On the other hand, higher temperatures suppress cooling in this model. For different β values, the temperature dependence is $t_{\rm cool} \propto F_T^{\beta+1/2}$. The cooling timescale only weakly depends on disk mass or pressure, via the logarithmic factor ξ. This weak dependence is a consequence of cooling coming from the radiative-convective boundary. Note that the scaling laws do not reflect the changes to ξ which remains order unity.

3.3.3. *Critical Core Mass*

We can define a critical more mass as that which gives a self-gravitating atmosphere within a typical gas disk lifetime:

$$t_{\rm cool} = 3 \times 10^6 \tau_{\rm cool} \text{ yr}, \quad (53)$$

with $\tau_{\rm cool}$ a scaling factor. The resulting critical core mass is

$$M_{\rm crit} \approx 100 \frac{F_T^{3/2} F_\kappa^{3/5} \left(\frac{\xi}{2.6}\right)^{6/5}}{\left(\frac{a_\oplus}{10}\right)^{\frac{9}{14}}} M_\oplus. \quad (54)$$

As with the cooling time, the critical mass is too large due to missing physics. The scaling with disk properties is similar, in fact all quantities are simply raised to the 3/5 power. The ξ value is changed to match the value for the nominal solution. The lower value reflects the fact that an atmosphere around such a massive core does not need to contract as much to be self-gravitating.

The numerical values for a different opacity law do not change the numerical answers above very much. That is mostly because we have chosen a disk location where $T_{\rm d}$ is not far from 100 K, where our opacity law is normalized. More generally a higher β value is more favorable for core accretion at large distances due to the sharper drop in opacity. The effects of opacity on the cooling time and critical core mass are discussed in appendix Appendix B

4. QUASI-STATIC KELVIN-HELMHOLTZ CONTRACTION **(PAPER I)**

In this section we describe our choices for the gas, disk and core parameters, and present some typical atmosphere numerical models. As mentioned in section 2.1, we assume that the central star is a Sun-like star with $M_* = M_\odot$. We are primarily interested in the outer regions of the protoplanetary disk, so we generate atmosphere models between 10 and 100 AU. As a fiducial case, we assume that the atmosphere is composed of a hydrogen-helium mixture with the helium mass fraction $Y = 0.3$., resulting in a mean molecular weight $\mu = 2.35$. We do not take into account the dependence of the adiabatic index on the helium fraction, and therefore assume the adiabatic index for a diatomic gas $\nabla_{\rm ad} = 2/7$. We further explore how the atmosphere evolution varies with adiabatic index and molecular weight. We generate model atmospheres for monatomic adiabatic index $\nabla_{\rm ad} = 2/5$ and for a purely molecular hydrogen composition ($\mu = 2$). The comparison between different gas compositions is deferred to section 5.4.

Figure 1 shows instantaneous atmosphere radial profiles at $a = 10$ AU accreting around a fixed core of mass $M_{\rm c} = 5M_\oplus$ for several total planet masses. In what follows, if the $R_B < R_H$ hierarchy holds, we define the planet mass as the total mass enclosed within the Bondi radius of the atmosphere, and regard the gas between the Bondi and Hill radii as perturbations due to the gravitational influence of the planet. For illustrative purposes we mark the position of the Bondi radius and of the radiative convective boundary. We notice that the pressure and temperature in the convective regions of the atmospheres scale as $1/r$, which is the expected behavior of an ideal gas adiabat with a polytopic equation of state (e.g., Rafikov 2006). In the outer radiative region of the atmosphere, the pressure has a nearly exponential profile, which is in agreement with the predictions of the analytic model (see section 3 and Appendix B). In addition, the atmosphere temperature at the radiative-convective boundary $T_{\rm RCB}$ only differs from the disk temperature $T_{\rm d}$ by an order unity factor, and so the atmosphere is nearly isothermal throughout the radiative zone. This is also in agreement with the analytic predictions.

The location of the Bondi radius moves further out as the mass of the atmosphere increases, as the Bondi radius scales with mass. The location of the radiative-convective boundary has a more interesting behavior. As stated in section 1, the nebular gas initially settles into equilibrium around the protoplanetary core on a short timescale relative to the thermal timescale, and is isen-

[2] The relevance of the neglected surface terms is discussed in Appendix B

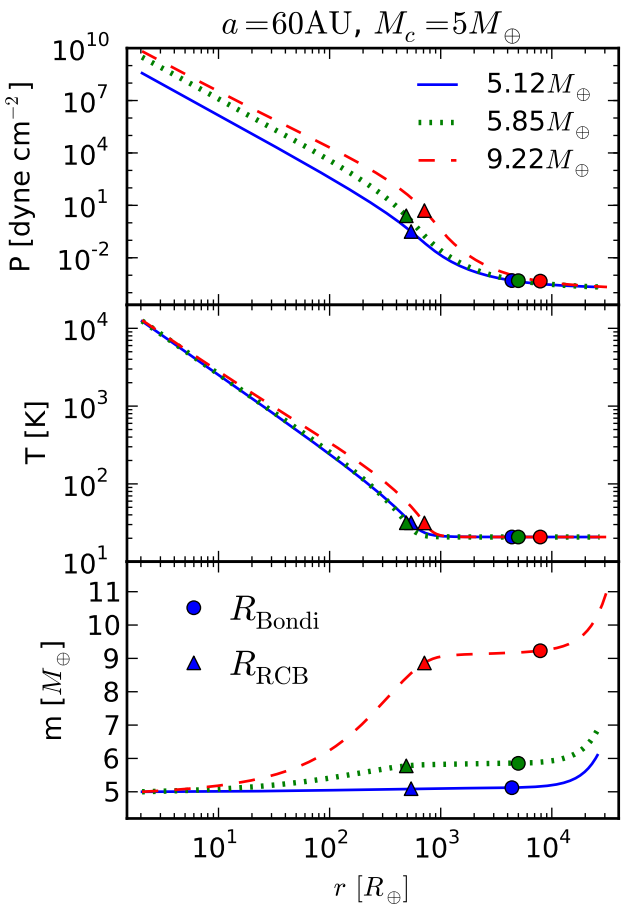

FIG. 1.— Example pressure, temperature and mass profiles as a function of radius.

tropic throughout with an entropy equal to that of the disk. In the context of our model, this atmosphere represents the minimum atmosphere mass for which a hydrostatic solution exists. This atmosphere is purely convective. As gas accumulates and the atmosphere starts cooling, an outer radiative region forms. This layer is thin for low mass atmospheres, as can be seen in Fig. 1: for the $5.21M_\oplus$ atmosphere, the ratio between the thickness of the radiative and convective regions is low. An increase in atmosphere mass causes the radiative zone to expand and the convective region to contract. As more and more gas is accumulated, the convective zone eventually starts expanding again; however, the ratio between the radii of the radiative and convective regions continually increases with atmosphere mass, i.e. the radiative regions of these types of atmospheres are getting deeper and deeper. [**This needs to be rephrased, somewhat vague and repetitive.**]

We further use the global cooling model developed in section 2.4 to obtain an evolutionary series from static atmosphere profiles. Figure 2 shows the luminosity and cooling time evolution with atmosphere mass. Gas accretion is initially rapid, but slows down significantly after a relatively small mass increase. For comparison, we also plot the analytic results derived in section 3. We see that there is only a very brief agreement between the analytic and full numerical results. At early times, the radiative zone is too shallow and so the approximation that $P_{\rm RCB} \gg P_{\rm d}$ used in section 3 breaks down. At late times, the self-gravity of the atmosphere becomes important.

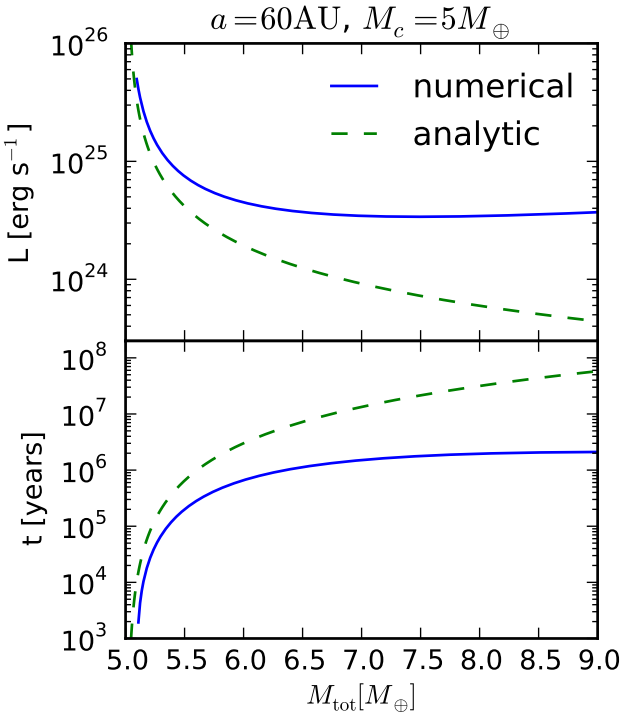

FIG. 2.— Luminosity and time evolution with mass. The analytic result is plotted for comparison.

4.1. *The End of Quasi-Static Evolution*

The right-hand side of equation (22) decreases with increasing atmosphere mass, and eventually becomes negative when the mass of the envelope becomes comparable to the core mass $M_{\rm atm} \sim M_{\rm c}$. This implies a negative luminosity from the RCB. Physically, the luminosity L represents the total heat flux through the surface defined by the RCB. The heat flux due to convective motions is always directed outwards, and hence it is positive. Moreover, the temperature gradient dT/dr is negative, as the temperature decreases towards the outside. As a result (see equation (8d)), the heat flux due to radiative diffusion is also positive. This implies that, in the absence of planetesimal accretion and internal heat sources, there is no physical mechanism that can justify a negative luminosity. The quasi-static, constant luminosity approximation breaks down at this point and a more detailed, time-dependent model is necessary.

5. CRITICAL CORE MASS **(PAPER I, EXCEPT FOR $\nabla_{\rm ad} = 2/5$ CASE)**

Standard static calculations of giant planet formation that consider planetesimal accretion as the main source of luminosity (e.g., Mizuno et al. 1978, Stevenson 1982, Rafikov 2006) assume that the atmosphere is at all times in a steady state at which the luminosity due to planetesimal accretion is fully radiated away by the atmosphere.

The core and the atmosphere grow simultaneously, and the mass of the envelope is a function of the core mass. As the atmosphere mass becomes comparable to the mass of the solid core, hydrostatic balance no longer holds and runaway gas accretion commences. Therefore, for a set of disk and gas conditions, there is a maximum mass the core can have before the onset of unstable accretion: this is defined as the critical core mass.

In our model the atmosphere is no longer in steady state, because energy balance requires gas accretion, and the atmosphere contracts on a Kelvin-Helmholtz time scale. Figure 3 shows the evolution of the atmosphere growth time with mass at several locations in our fiducial disk for a fixed core mass. In the early stages when $M_{\rm atm}$ is small, the envelope has a thin radiative zone and hence a high luminosity (see Figure 2). As a result, the envelope initially grows quickly, as shown in Figure 3. As the radiative zone becomes thicker, the luminosity decreases and growth slows down. For our choice of parameters, we see that accretion is slowest for an atmosphere mass of $1-2M_\oplus$. This is when the self-gravity of the atmosphere starts to matter; the envelope becomes massive enough for its energy to be large compared to the internal energy of the nebular gas. As a result, growth is continuously accelerated, and eventually runaway gas accretion settles in when the mass of the atmosphere becomes comparable to the core mass. Since growth is slowest before $M_{\rm atm} \sim M_{\rm c}$ for the cases that we tried, the estimate of the time to initiate runaway gas accretion is insensitive to the exact choice of crossover atmosphere mass to order of magnitude. We therefore choose the effective crossover mass, past which hydrostatic balance no longer holds, to be the minimum between $M_{\rm c}$ and the $M_{\rm atm} < M_{\rm c}$ at which our model becomes unphysical according to equation (22), noting that both of these occur after the slow accretion phase for all our parameter choices. We define the *crossover time* $t_{\rm co}$ as the time elapsed until the atmosphere mass becomes equal to the effective crossover mass as defined above, and runaway accretion commences.

In this section we explore the dependence of the crossover time on core, disk and gas parameters, and determine the minimum core mass needed to initiate runaway gas accretion within the lifetime of the protoplanetary disk. In section 5.1 we show the dependence of the crossover time on the core mass at a fixed distance in the disk, justifying the need for a "minimum" core mass. We further explore how the crossover time is affected by the position in the disk in section 5.2 and by the mean molecular weight and opacity of the nebular gas in section 5.3. Finally, we determine the minimum core mass necessary for a giant planet to form before the nebular gas dissipates; we define this minimum mass as the *critical core mass* for runaway accretion to commence.

5.1. *Influence of Core Mass on Crossover Time*

We begin by fixing the disk properties and generating atmosphere profiles for a set of fixed core masses. Figure 4 shows the crossover time behavior for a range of cores with masses between 1 and 10 $M_\oplus$, at $a = 10$ AU in our fiducial disk. The envelope grows faster if the core is more massive, as it can bind a gaseous atmosphere more quickly due to larger gravity. This can also be seen from the analytical results in equation (52). As such,

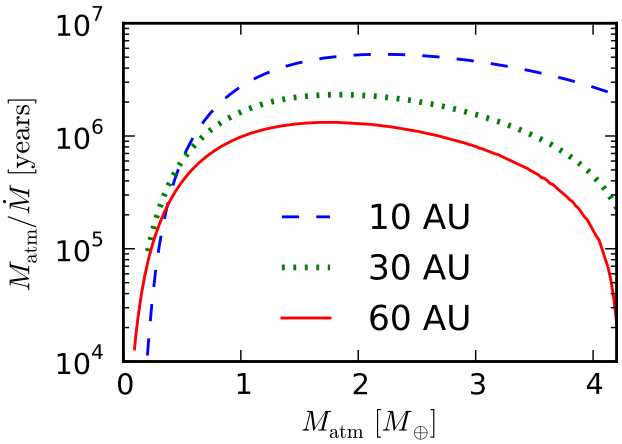

FIG. 3.— Instantaneous growth time for the atmosphere of a planet with fixed core mass $M_{\rm c} = 5M_\oplus$ as a function of atmospheric mass, for a planet located at 10, 30 and 60 AU. Accretion is slowest before the mass of the atmosphere becomes comparable to the mass of the core. In this example, this happens at $M_{\rm atm} \sim 1-2M_\oplus$.

for a fixed crossover time, e.g. the typical lifetime of the protoplanetary disk, there is a minimum core mass needed to form a planet within this time frame, which we defined above as the critical core mass. We defer numerical estimates of the critical core mass to section 5.4.

We also find that the atmosphere growth time is very sensitive to the core mass: for the choice of parameters in Figure 4, the mass increase needed to reduce the crossover time by a factor of two is only half an Earth mass.

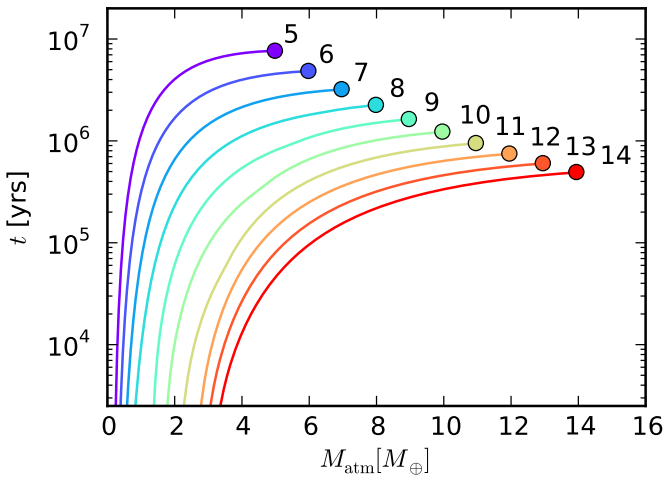

FIG. 4.— We generate atmosphere profiles at $a = 10$ AU for cores with fixed masses between $5M_\oplus$ and $14M_\oplus$. We plot the cumulative cooling time as a function of atmosphere mass. The circles mark the crossover time. A larger core mass results in a shorter crossover time.

5.2. *Role of Disk Temperature and Pressure*

In what follows we explore how the crossover time is affected by the planet's location in the disk. The location only matters because it dictates the disk temperature (equation (1b)) and pressure (equation (2)). We therefore study the separate effects of disk temperature and pressure on the time evolution of the atmosphere. At a fixed distance in the disk $a = 10$ AU and for a core mass $M_c = 5M_\oplus$, we fix the disk temperature T_d at the value given by equation (1b) and vary the disk pressure P_d. We perform a similar analysis on the effect of disk temperature T_d on the crossover time by fixing the disk pressure at the value given by equation (2) and varying T_d. The resulting time evolution is plotted in Figure 5. For comparison, we also plot the results predicted by the analytic, non self-gravitating model described in section 3. However, we saw in equation (52) that the crossover time as predicted by the analytic results is too long. Here we are investigating whether the analytic model predicts the correct scalings as opposed to the actual absolute results, when compared to the numerical model. We therefore estimate the analytic crossover time as the time needed for the atmosphere to reach an effective crossover mass $M_{atm} = fM_c$, where $f = 0.13$.

We find that the crossover time is shorter for lower disk temperatures and higher pressures. We discuss the two effects separately.

An increase in disk temperature results in a longer crossover time, as a higher temperature causes an increase in opacity and hence a lower luminosity. The analytic model predicts $t_{co} \propto T^{\beta+1/2}$ (see equation (52)), where β is the constant in the opacity law (14). For our choice of $\beta = 2$, the crossover time is therefore strongly dependent on the opacity. Different opacity assumptions will result in a different scaling with temperature of t_{co}. We notice a generally good agreement between our numerical results and the scaled analytic approximation in the left panel of Figure 5. A factor of ~ 3 reduction in the disk temperature results in an decrease of the growth time by a factor of ~ 30. The atmosphere evolution is therefore strongly dependent on the temperature in the protoplanetary disk.

An increase in disk pressure will decrease the crossover time. This effect can also be explained by the analytic model. From equations (52) and (49), the crossover time is inversely proportional to the disk pressure. A higher disk pressure will therefore result in a shorter crossover time. Increasing the disk pressure by a factor of ~ 100 only reduces the crossover time by a factor of ~ 2. As such, the crossover time is only weakly dependent on the nebular pressure.

5.3. *Role of Mean Molecular Weight and Opacity*

In this work we build evolutionary atmosphere profiles assuming an ideal gas equation of state with constant mean molecular weight and adiabatic index. A realistic gas mixture, however, has variable adiabatic gradient and molecular weight, due to non-ideal effects and processes like dissociation or ionization. Future work will include real gas equation of state tables, and we expect quantitatively different results. In this study we analyze only the effect of the mean molecular weight of the nebular gas on the crossover time. In Figure 6, we compare our standard model given by $\nabla_{ad} = 2/7$ and $\mu = 2.35$ with a model with the same adiabatic index but a different molecular mass, $\mu = 2$ (i.e., purely molecular hydrogen). We also plot the analytic results for comparison, using the same fractional mass scaling as in subsection 5.2, $f = 0.13$, and notice that they are in good agreement with the numerical models. A lower mean molecular weight translates into a longer crossover time for the same core mass, since an atmosphere composed of heavier molecules is easier to bind.

A decrease in opacity reduces the number of steps that photons need to diffuse (since it increases their mean free path), resulting in a higher luminosity. In Figure 7, we explore opacity laws in which the coefficient κ_0 from equation (14) is reduced by factors of 10 and 100. All things equal, a lower opacity increases the luminosity and hence speeds atmosphere growth by the same factor as the opacity reduction (see equations (8d) and (9)).

5.4. *Critical Core Mass*

We can now combine the results obtained in sections 5.1, 5.2 and 5.3 to determine the minimum core mass necessary for a protoplanet to initiate runaways gas accretion within the disk lifetime, i.e. to have a crossover time equal to the disk life timescale. We denote this mass the *critical core mass*.

Observations of protoplanetary disks show that they dissipate over a time scale of a few million years (e.g., Lagrange et al. 2000, Haisch et al. 2001, Goldreich et al. 2004). We adopt a disk life timescale of $\tau = 3$ Myrs and determine the critical core mass as a function of gas and disk conditions.

In Figure 8, we see that the critical core mass decreases as we move further away in the disk, primarily due to the fact the disk temperature is lower in the outer regions of the disk. As we showed in section 5.2, the atmosphere grows faster for lower temperatures, which offsets the need for a larger core mass. The critical core mass is larger for a lower mean molecular weight, consistent with the results derived in section 5.1. **Add explanation for analytic curve behavior — need to chat about this with Andrew**. We also explore the opacity effect on the critical core mass in Figure 9 For an opacity, and therefore crossover time, reduced by an order of magnitude, the critical core mass is reduced by roughly a factor of 2.

6. DISCUSSION

In this section we discuss the parameter space of validity of our model. We calculate the conditions under which planetesimal accretion can be ignored, and review the effects of some of the approximations that come into our model.

6.1. *Comparison with Planetesimal Accretion* ***(Paper II)***

In this study we have considered atmospheres for which planetesimal accretion is negligible and Kelvin-Helmholtz contraction dominates the luminosity evolution of the atmosphere. This is different from standard calculations, in which the atmosphere is heated by planetesimal accretion. In this section we investigate the core accretion rates that are necessary for our regime to be valid. We also discuss the conditions under which runaway gas accretion can be initiated due to the Kelvin-

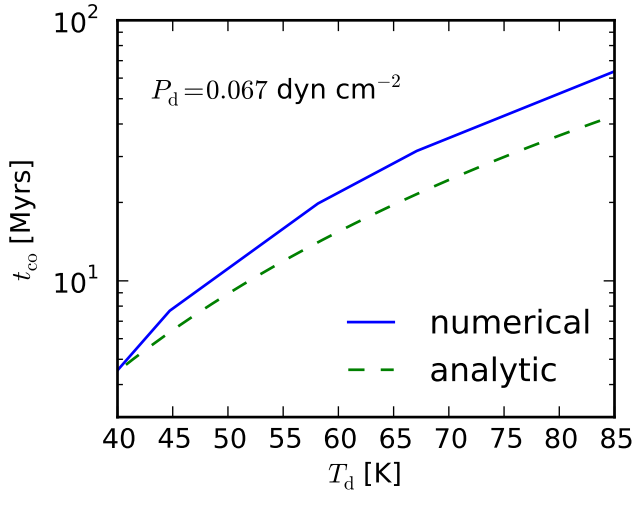

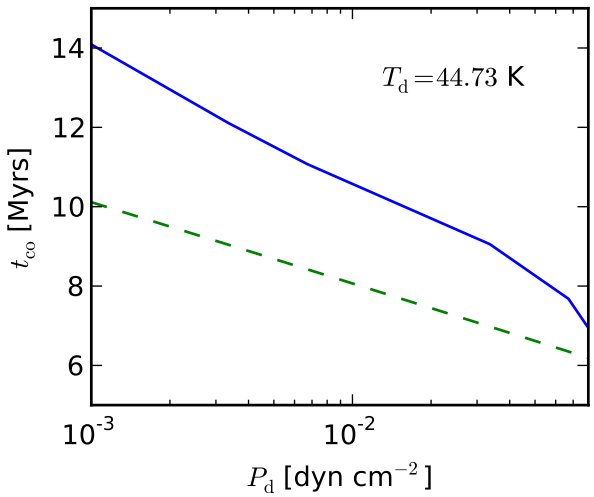

FIG. 5.— Left panel: crossover time as a function of disk temperature for fixed disk pressure and a core of fixed mass $M_{\rm c} = 5M_{\oplus}$. Right panel: crossover time as a function of disk pressure for fixed disk temperature and a core of fixed mass $M_{\rm c} = 5M_{\oplus}$. The analytic scalings are plotted for comparison, for an effective crossover mass $M_{\rm co} = fM_{\rm c}$ with $f = 0.13$. Gas accretion is faster for lower temperatures and higher pressures.

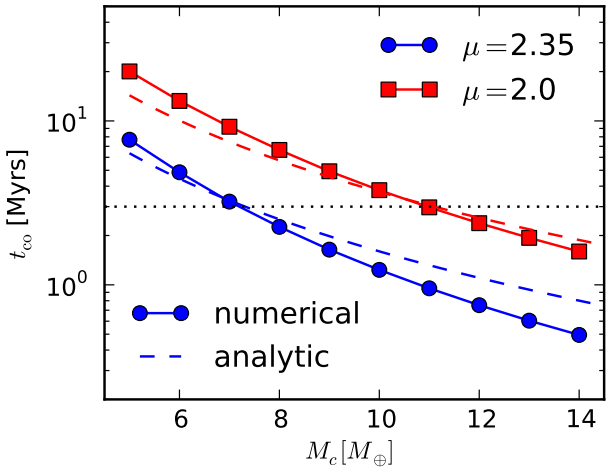

FIG. 6.— The crossover time $t_{\rm co}$ as a function of core mass at $a = 10$ AU, for atmospheres with different mean molecular weight. A typical protoplanetary disk life time $t = 3$ Myrs is plotted for comparison. The crossover time is larger for a lower mean molecular weight.

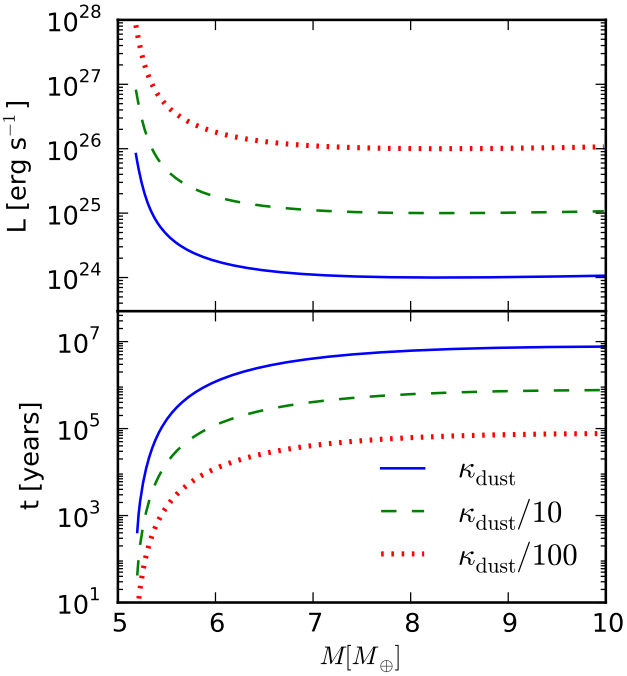

FIG. 7.— Luminosity and cooling time evolution with total atmosphere mass for planets of fixed core mass $M_{\rm c} = 5M_{\oplus}$ and located at $a = 10$ AU, for different opacities. The standard dust opacity is reduced by factors of 10 and 100, respectively. A lower opacity accelerates atmosphere growth.

Helmholtz contraction of the atmosphere before it becomes critical due to planetesimal accretion.

We estimate the planetesimal accretion rate consistent with our assumptions that $L_{\rm acc} \ll L_{\rm KH}$. Here $L_{\rm acc}$ is the accretion luminosity given by

$$L_{acc} = G\frac{M_{\rm c}\dot{M}_{\rm c}}{R_{\rm c}}, \qquad (55)$$

where $\dot{M}_{\rm c}$ is the core accretion rate, and $L_{\rm KH}$ is the luminosity of the atmosphere due to gas contraction as calculated in section 4. At the limit, $L_{\rm acc} = L_{\rm KH}$. For a given atmosphere model we can therefore estimate the maximum planetesimal accretion rate during the gas contraction phase in order for the atmosphere to be dominated by the Kelvin-Helmholtz luminosity. We choose as a fiducial case an atmosphere forming at 10 AU and with a core mass of $10M_{\oplus}$. For this choice or parameters, the atmosphere cooling time is ~ 1.2 Myrs (see Figure 7), which is within the typical life time of a protoplanetary

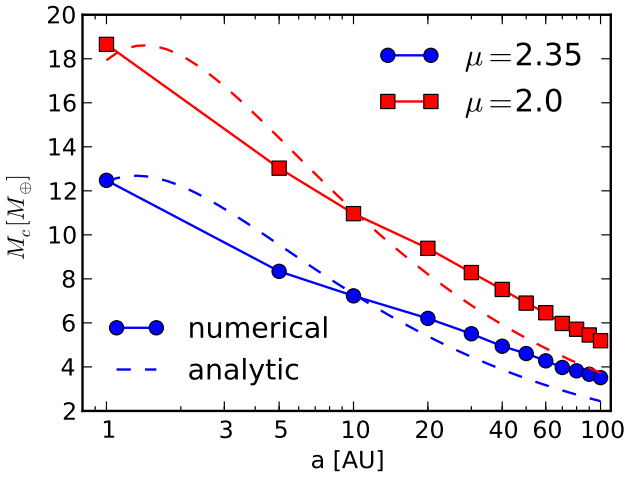

FIG. 8.— The minimum core mass for an atmosphere to initiate runaway gas accretion within the lifetime of the disk $t \sim 3Myrs$ as a function of semi-major axis, for different mean molecular weight of the nebular gas. The analytic results are plotted for comparison. The critical core mass is lower further out in the disk.

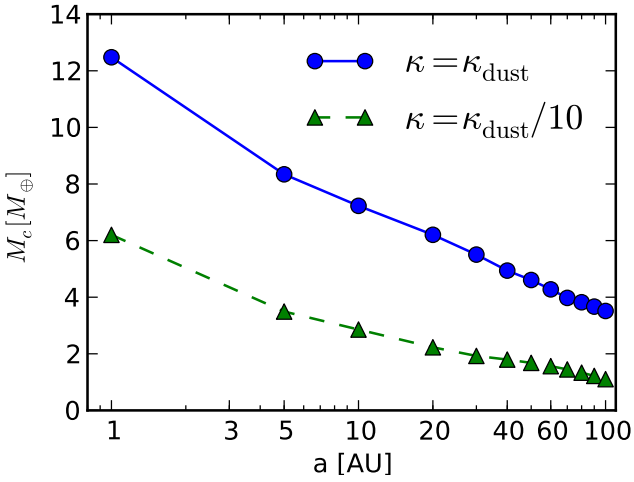

FIG. 9.— Critical core mass as a function of semi-major axis for different opacities. A factor of ten opacity reduction results in a critical core mass twice as small.

disk. The results are presented in Figure 10.

We label the resulting minimum core accretion rate as $\dot{M}_{\rm c,KH}$. The atmosphere growth rate is also plotted for comparison. We therefore see that the core accretion rate has to be $\sim 2-3$ orders of magnitude lower than the atmosphere accretion rate for our assumptions to be valid. If the core had accreted planetesimals at this constant rate since it started forming, then the formation of a core massive enough to attract an atmosphere would not have been possible within typical disk life timescales, which indicates a slowing down of the planetesimal accretion regime. Possible explanations for that include the core having formed in the inner part of the disk and later migrated outwards, or the core having been depleted of planetesimals due to a giant neighbor. We also estimate the core accretion rate

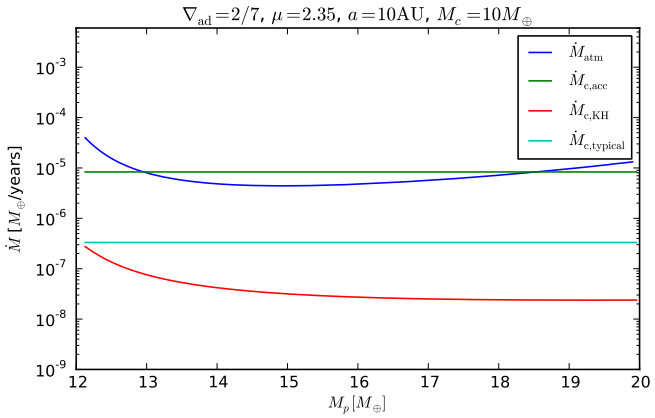

FIG. 10.— Various relevant accretion rates. $\dot{M}_{\rm atm}$ is the growth rate of the atmosphere as estimated by our model, and $\dot{M}_{\rm c,KH}$ is the maximum planetesimal accretion rate during the gas contraction phase in order for our regime to be valid. For comparison, we plot the core accretion rate $\dot{M}_{\rm c,acc}$ necessary to grow the core on the same time scale as the atmosphere $\tau \sim 1.2$ Myrs, and a typical planetesimal accretion rate where the random velocity of the planetesimals is given by the Hill velocity due to the core.

$$\dot{M}_{\rm c,acc}(M_{\rm c}) \equiv \frac{M_{\rm c}}{\tau} \tag{56}$$

needed for the core to form on the same timescale as our model atmosphere, $\tau = 1.2$ Myrs, as well as a typical planetesimal accretion rate, for which the random velocities of the planetesimals are of the order of the Hill velocity around the protoplanetary core (Goldreich et al. 2004). We denote this latter rate as $\dot{M}_{\rm c,typical}$. This rate, which is at the boundary of the dispersion dominated and shear dominated regimes ,is often quoted as a maximum (refs). However, it is easy to see that $\dot{M}_{\rm c,typical}$ is more than one order of magnitude lower than the gas accretion rate of our model atmosphere $\dot{M}_{\rm atm}$, and lower than the core accretion rate $\dot{M}_{\rm c,acc}$ needed to grow the core and the atmosphere at the same time within the disk life time. As such, the formation of a giant planet by growing the core first, then letting the atmosphere cool is faster than growing the core and the atmosphere at the same time at a steady planetesimal accretion rate.

Next, we are interested in whether hydrodynamic gas accumulation due to planetesimal accretion can already commence before the atmosphere becomes unstable due to Kelvin-Helmholtz contraction, as our regime is no longer the relevant one under such conditions. A core that forms on the same timescale as our model atmosphere accretes planetesimals at a rate given by equation (56). This accretion rate is dependent on the core mass, which is steadily increasing. We therefore compare the critical core mass due to planetesimal accretion at this rate $M_{\rm crit,acc}$ to a core mass assumed fixed $M_{\rm c,fixed}$. If $M_{\rm crit,acc} < M_{\rm c,fixed}$, then the atmosphere has already initiated unstable gas accretion by the time Kelvin-Helmholtz contraction starts dominating.

In order to estimate the critical core mass due to planetesimal accretion $M_{\rm crit,acc}$, we use the results of Rafikov (2006) for low luminosity atmospheres forming in the outer disk ($> 2-5$ AU), consistent with our region of

interest. By relating his expression for the critical core mass to a given core mass dependent planetesimal accretion rate $\dot{M}(M_c)$, we find the following expression for the critical core mass when accretion luminosity dominates the evolution of the atmosphere:

$$M_{\rm crit,acc} \sim \left[\frac{\dot{M}(M_c)}{64\pi^2}\frac{\kappa_0}{\sigma G^3}\frac{1}{R_c M_c^{1/3}}\left(\frac{k}{\mu}\right)^4\right]^{3/5}, \quad (57)$$

with all the constants as defined in previous sections. We therefore calculate $M_{\rm crit,acc}$ for a range of core masses. The result is displayed in Figure 11.

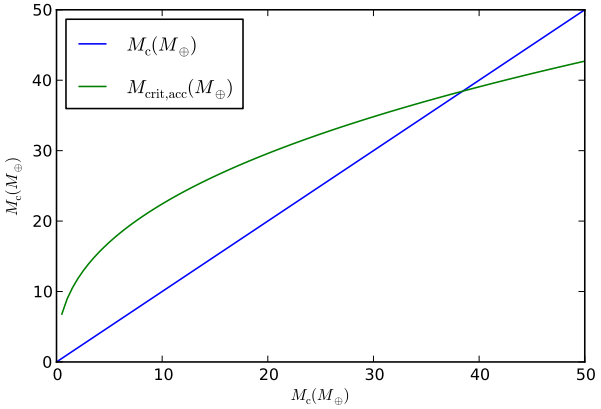

FIG. 11.— Comparison between the critical core mass $M_{\rm crit,acc}$ due to planetesimal accretion and the assumed fixed core mass when gas contraction dominates, for a growth time of $\tau = 1.2$ Myrs. Unstable atmosphere collapse occurs due to core accretion before Kelvin-Helmholtz contraction starts dominating for core masses larger than $\sim 40 M_\oplus$.

We see that the critical core mass due to planetesimal accretion is smaller than the mass of the fixed core for $M_c \sim 40 M_\oplus$. This means that for large core masses, planetesimal accretion will lead to runaway gas accretion before gas contraction starts dominating, and hence our model is not applicable in that regime. However, we have found in section 5.4 that unstable atmospheres collapse occurs within the life time of the disk for protoplanetary cores smaller than this. We therefore confirm that planetesimal accretion can be safely ignored in our regime of interest. Moreover, as displayed in Fig. 10, it is faster to form a planet by growing the core first, then accreting a massive envelope, rather than by growing the core and atmosphere in parallel. **This works for this particular choice of core, disk etc. conditions, and I am expecting it to work for most of our parameter space, but it would probably be good to explore this numerically, at least to order of magnitude, with the estimates we have.**

As a final check, we investigate whether planetesimal accretion during the gas contraction phase at the rate $\dot{M}_{\rm KH}$ imposed by the condition that $L_{\rm acc} < L_{\rm KH}$ can alter the core mass enough to affect the time evolution of the atmosphere. We can quantitatively estimate the increase in core mass as

$$\Delta M_c = \int_0^{t_{\rm crit}} \dot{M}_c dt \approx \sum_i \dot{M}_{ci}\Delta t_i, \quad (58)$$

where $t_{\rm crit}$ is the time elapsed until runaway gas accretion commences, and the accretion rate $\dot{M}_{ci}$ is given by

$$\dot{M}_{ci} = \frac{L_i R_c}{G M_c} \quad (59)$$

from equation (55), with L_i the luminosity of the atmosphere at time t_i in our model. For $M_c = 10 M_\oplus$, we find $\Delta M_c \approx 0.05 M_\oplus$. This mass increase is therefore negligible in comparison with the initial core mass. It follows that a significant increase in core mass that could potentially alter the time evolution of the atmosphere would occur on a longer time scale than the mass-doubling time for the unperturbed atmosphere. Therefore, the time evolution of the atmosphere is insensitive to core mass changes at a rate imposed by the assumption that $L_{\rm acc} < L_{\rm KH}$.

6.2. *Neglected Effects*

In this section we summarize some of the simplifications we have made, and discuss their relative effect on our model.

6.2.1. *Equation of State* ***(Paper II)***

In our model we assume an ideal gas law and a polytropic equations of state (EOS), given by equations (13) and (12), respectively. However, non-ideal effects such as partial dissociation and ionization have to be taken into account. One solution is using tabulated equation of state tables for hydrogen and helium mixtures. As future work, we plan to use the Saumon et al. (1995) EOS tables and extend them to lower pressures and temperatures as required by our disk assumptions.

6.2.2. *Time Evolution* ***(Paper I)***

In this study we have assumed that the luminosity stays constant throughout the radiative region of the atmosphere. As a result, the time dependence can be neglected in equation (8d) and static solution can be obtained and then connected through a global cooling equations, as described in section 2.4. However, the assumption of constant luminosity breaks down for high atmosphere masses, as described in section 4.1; in this case, a time-dependent model is required to describe the atmosphere evolution. We are currently developing a full evolutionary time-dependent atmosphere model. We do not expect qualitatively different results. We showed in section 4.1 that the quasi-static model breaks down around the time when the atmosphere mass becomes equal to the mass of the core. Nevertheless, we can see from Figures 2 and 3 that the time of slowest accretion is safely before the region in which our model breaks down, and that the time after which the atmosphere mass increases by 25 % is only a factor of 2 lower than the mass doubling time. As a result, we are confident of our results to order of magnitude.

6.2.3. *Inefficient Convection****(Paper I)***

Discussion about mixing length theory...

6.2.4. *Opacity* ***(Paper II)***

In progress, still need to run models for smaller AU and see at what point ice grain opacity is

no longer valid. Currently strange behavior at 1 AU for $\nabla_{\rm ad} = 2/5$, the critical core mass goes up significantly instead of having a linear trend. $\nabla_{\rm ad} = 2/7$ atmospheres do not show this effect. Models for the inner disk would also show / confirm that close-in giant planet formation is hard (need larger core mass).

7. CONCLUSIONS

In this paper we have studied the formation of giant planet atmospheres under the assumption that Kelvin-Helmoholtz gas contraction dominates the luminosity evolution of the atmosphere over planetesimal accretion. We built quasi-static two-layer atmosphere models with an inner convective region and an outer radiative region that matches smoothly onto the protoplanetary disk. We derived a cooling model to connect series of quasti-static atmospheres, and thus obtained an evolutionary history of the envelope. We defined the time at which unstable atmosphere collapse commences as $M_{\rm atm}(t) \sim M_{\rm c}$. From this we defined as "critical core mass" the minimum core mass for a protoplanet to initiate runaway gas accretion during the lifetime of the protoplanetary disk. We studied this minimum mass for a variety of disk conditions, nebular gas compositions and opacities. We found that the critical core mass decreases as we move further out in the disk, and is smaller for lower disk temperatures and opacities and for higher mean molecular weight of the gas.

We find that the critical core mass to form a giant planet within the life time of the disk is smaller than the results yielded by studies that assume that the atmosphere evolution is dominated by the luminosity due to planetesimal accretion. We have showed that the planetesimal accretion rate needed to grow the core on a typical disk time scale is larger than the expected planetesimal accretion rates at large separations. As such, it is faster to form a planet by growing the core first in a fast planetesimal accretion regime (e.g., the core forms in the inner disk, then migrates outwards), then significantly reduce planetesimal accretion and allow a massive atmosphere to accumulate.

REFERENCES

Bell, K. R. & Lin, D. N. C. 1994, ApJ, 427, 987
Chiang, E. & Youdin, A. N. 2010, Annual Review of Earth and Planetary Sciences, 38, 493
D'Angelo, G., Durisen, R. H., & Lissauer, J. J. Giant Planet Formation, ed. S. Piper, 319–346
Goldreich, P., Lithwick, Y., & Sari, R. 2004, ARA&A, 42, 549
Haisch, Jr., K. E., Lada, E. A., & Lada, C. J. 2001, ApJ, 553, L153
Ikoma, M., Nakazawa, K., & Emori, H. 2000, ApJ, 537, 1013
Kippenhahn, R. & Weigert, A. 1990, Stellar Structure and Evolution
Lagrange, A.-M., Backman, D. E., & Artymowicz, P. 2000, Protostars and Planets IV, 639
Mizuno, H., Nakazawa, K., & Hayashi, C. 1978, Progress of Theoretical Physics, 60, 699
Papaloizou, J. C. B. & Nelson, R. P. 2005, A&A, 433, 247
Papaloizou, J. C. B. & Terquem, C. 1999, ApJ, 521, 823
Rafikov, R. R. 2005, ApJ, 621, L69
—. 2006, ApJ, 648, 666
Saumon, D., Chabrier, G., & van Horn, H. M. 1995, ApJS, 99, 713
Semenov, D., Henning, T., Helling, C., Ilgner, M., & Sedlmayr, E. 2003, A&A, 410, 611
Stevenson, D. J. 1982, Planet. Space Sci., 30, 755
Thompson, M. J. 2006, An introduction to astrophysical fluid dynamics
Wuchterl, G. 1993, , 106, 323

APPENDIX

DERIVATION OF GLOBAL ENERGY EQUATION

We derive here the global energy equation (16). We follow the simpler example in §4.3 of Kippenhahn & Weigert (1990), adding the effects of finite core radius, surface pressure and mass accretion. We assume that hydrostatic balance holds. Integrating the local energy equation (19) from core to surface gives:

$$L - L_{\rm c} = \int_{M_{\rm c}}^{M} \frac{\partial L}{\partial m} dm \tag{A1a}$$

$$= \int_{M_{\rm c}}^{M} \left(\epsilon - T \frac{\partial S}{\partial t} \right) dm \tag{A1b}$$

$$= \Gamma - \int_{M_{\rm c}}^{M} \frac{\partial u}{\partial t} dm + \int_{M_{\rm c}}^{M} \frac{P}{\rho^2} \frac{\partial \rho}{\partial t} dm \,. \tag{A1c}$$

with $\Gamma = \int \epsilon dm$ the integral of the direct heating rate.

In what follows, we must carefully distinguish between partial time derivatives, $\partial/\partial t$, (performed at fixed mass) and total time derivatives, denoted with overdots (which include the effect of mass accreted through the outer boundary). For instance the surface radius, R, evolves as

$$\dot{R} = \frac{\partial R}{\partial t} + \frac{\dot{M}}{4\pi R^2 \rho_M} \tag{A2}$$

where $\partial R/\partial t$ gives the Lagrangian contraction of surface mass elements, and $\dot{M}$ denotes mass accretion rate through the upper boundary. The subscript M denotes quantities at the upper boundary of total mass M (though it is omitted

from M and R). Similarly the volume, $V = (4\pi/3)r^3$ and pressure at the surface evolve as

$$\dot{V}_M = \frac{\partial V_{\rm M}}{\partial t} + \frac{\dot{M}}{\rho_{\rm M}} \tag{A3a}$$

$$\dot{P}_M = \frac{\partial P_{\rm M}}{\partial t} + \frac{\partial P_M}{\partial m}\dot{M} \tag{A3b}$$

$$= \frac{\partial P_{\rm M}}{\partial t} - \frac{GM}{4\pi R^4}\dot{M}\,. \tag{A3c}$$

For the purpose of this derivation we will hold the core mass fixed $\dot{M}_{\rm c} = 0$ which further gives $\dot{P}_{\rm c} = \partial P_{\rm c}/\partial t$.

To derive the global energy equation we must move the (partial) time derivatives in Equation (A1c) outside their integrals. The internal energy integral follows simply from Leibniz's rule as

$$\int_{M_{\rm c}}^{M(t)} \frac{\partial u}{\partial t} dm = \dot{E}_i - \dot{M} u_M\,. \tag{A4}$$

To evaluate the work integral, we derive a pair of expressions for the rate of change of gravitational energy. The time derivative of Equation (20) gives

$$\dot{E}_G = 3\int_{M_{\rm c}}^{M} \frac{P}{\rho^2}\frac{\partial \rho}{\partial t} dm - 3\int_{M_{\rm c}}^{M} \frac{\partial P}{\partial t}\frac{dm}{\rho} \tag{A5}$$
$$-3\frac{P_M}{\rho_M}\dot{M} + 3\dot{P}_M V_M - 3\dot{P}_{\rm c} V_{\rm c} + 3P_M \dot{V}_M\,.$$

The first integral in Equation (A5) is the one we want, but the next one must be eliminated. The time derivative of Equation (17) (times four) gives

$$4\dot{E}_G = -4\frac{GM\dot{M}}{R} + 4\int_{M_{\rm c}}^{M} \frac{Gm}{r^2}\frac{\partial r}{\partial t} dm \tag{A6a}$$

$$= -4\frac{GM\dot{M}}{R} + 4\pi\int_{M_{\rm c}}^{M} r^3 \frac{\partial}{\partial m}\frac{\partial P}{\partial t} dm \tag{A6b}$$

$$= -4\frac{GM\dot{M}}{R} - 3\int_{M_{\rm c}}^{M} \frac{\partial P}{\partial t}\frac{dm}{\rho} \tag{A6c}$$
$$+3V_M\frac{\partial P_M}{\partial t} - 3V_{\rm c}\frac{\partial P_{\rm c}}{\partial t}$$

where Equations (A6b) and (A6c) use hydrostatic balance and integration by parts.

Subtracting Equations (A4) and (A6c) and rearranging for the desired integral gives

$$\int_{M_{\rm c}}^{M} \frac{P}{\rho^2}\frac{\partial \rho}{\partial t} dm = -\dot{E}_G - \frac{GM\dot{M}}{R} - P_M\frac{\partial \dot{V}_M}{\partial t} \tag{A7}$$

with Equation (A3) used to combine terms. Combining Equations (A1c), (A4) and (A7), we reproduce Equation (16) with the accreted energy $e_{\rm acc} \equiv u_M - GM/R$.

ANALYTIC COOLING MODEL DETAILS

Estimate of Atmosphere Mass Outside the Bondi Radius

Here we consider the mass exterior to the Bondi radius. For a meaningful evaluation we only include the mass coming from the overdensity relative to the background density. The resulting external mass for an isothermal atmosphere is

$$M_{\rm ext} = 4\pi\int_{R_{\rm B}}^{r_{\rm fit}} (\rho - \rho_{\rm o}) r^2 dr \tag{B1a}$$

$$= M_{\rm c}\theta_{\rm c}\int_1^{n_{\rm fit}} 3\left[\exp\left(\frac{1}{x} - \frac{1}{n_{\rm fit}}\right) - 1\right] x^2 dx$$

$$\equiv M_{\rm c}\theta_{\rm c} I(n_{\rm fit}) \tag{B1b}$$

where $\theta_c = R_B/R_{\rm c}$ and the dimensionless integral $I(n_{\rm fit})$ obeys the limits $I(1) = 0$ and $I \to n_{\rm fit}^2/2$ as $n_{\rm fit} \to \infty$. Since this external mass does not converge, the choice of an outer boundary does matter in principle. In practice, however,

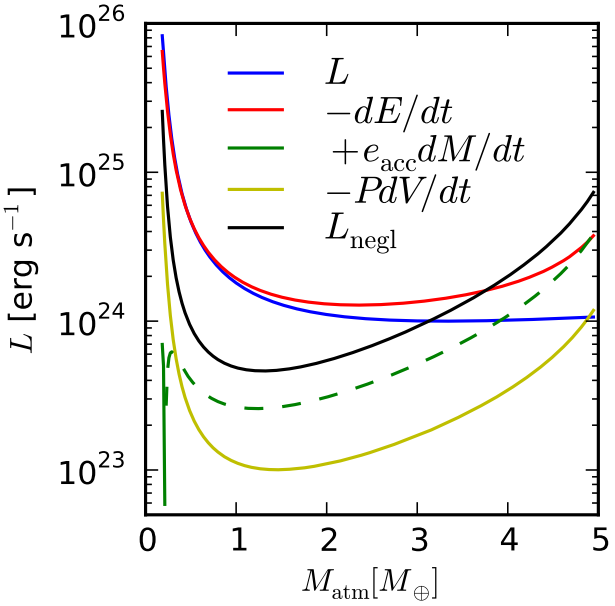

FIG. 12.—

the assumption that $r_{\rm fit} = R_{\rm H}$ limits $n_{\rm fit}$ to modest values

$$n_{\rm fit} = \frac{R_{\rm H}}{R_{\rm B}} \approx 1.3 \frac{a_{10\oplus}^{4/7}}{m_{\rm c10\oplus}^{2/3}} \frac{F_T}{m_*^{1/3}}. \tag{B2}$$

Since for instance $I(2) = 1.1$, these modest $n_{\rm fit}$ values will only produce a small external mass.

The Opacity Effect

A lower opacity could lower the core mass. Reducing the opacity by a factor of one hundred cuts the core mass by more than a factor of 10, specifically to 9 $M_\oplus$ for the parameters in Equation (54). The reduction is not as strong as the nominal scaling would imply, $0.01^{3/5} \approx 0.06$, because ξ increases.

Even with significantly lower opacities, radiative diffusion remains a good approximation at the radiative-convective boundary. We estimate the optical depth as (for $\beta = 2$):

$$\tau_{\rm RCB} \sim \frac{\kappa P_{\rm RCB}}{g} \sim 7 \times 10^4 \frac{F_T^4 F_\kappa}{\left(\frac{m_{\rm c}\oplus}{10}\right)\left(\frac{a_\oplus}{10}\right)^{\frac{12}{7}}} \tag{B3}$$

where $P_{\rm RCB} \sim P_M$ for a self-gravitating atmosphere and $g \sim GM_{\rm c}/R_B^2$, with both approximation good to within the the order unity factor ξ. Clearly $\tau_{\rm RCB} \gg 1$ even for $F_\kappa \lesssim 0.01$ out to very wide separations.

A hotter disk would increase core masses. Instead of our passive disk model, adopting the standard Hayashi temperature profile would increase core masses by $\sim 50\%$. A hotter accretion phase would further increase core masses, but such phases are presumably short lived.

Surface Terms

We now check the relevance of the neglected surface terms in Equation (16). We already showed that accretion energy can be exactly eliminated by choosing an outer boundary near the Bondi radius. We now show that accretion energy is also a small correction at the RCB. A rough comparison, (ignoring terms of order ξ) of accretion luminosity vs. $\dot{E}$ gives

$$\frac{GM\dot{M}}{R\dot{E}} = \frac{GM}{R}\frac{dM}{dE} \sim \frac{GM_{\rm c}^2}{R_B E}\frac{P_{\rm RCB}}{P_M} \sim \sqrt{\frac{R_{\rm c}}{R_B}} \ll 1, \tag{B4}$$

where we assume $P_{\rm RCB} \sim P_M$ for a massive atmosphere. Accretion energy at the protoplanetary surface is thus very weak for marginally self-gravitating atmospheres, and even weaker for lower mass atmospheres. A similar scaling analysis shows that the work term, $P_M \partial V_M/\partial t$ is similarly weak. Nevertheless our numerical calculations include these surface terms in a more realistic and complete model of self-gravitating atmospheres.

TABLE 1
PARAMETERS DESCRIBING STRUCTURE OF RADIATIVE ZONE.

$\gamma = 7/5$ ($\nabla_{\rm ad} = 2/7$), $\alpha = 0$					
β	1/2	3/4	1	3/2	2
∇_∞	2/7 [a]	4/13	1/3	2/5	1/2
χ	···	2.25245	1.91293	1.65054	1.52753
θ	···	0.145032	0.285824	0.456333	0.556069

[a] Since $\nabla_{\rm ad} = \nabla_\infty$ there is no convective transition at depth for this case.

Hydrogen Dissociation

The dissociation of molecular hydrogen deep in the atmospheres of accreting protoplanets plays a significant role in the energetics of core accretion. In the high density regions $r \ll R_{\rm RCB}$ of a convective atmosphere, the thermal plus gravitational energy scales as

$$dE = -4\pi\nabla_{\rm ad}^{1/\nabla_{\rm ad}}\rho_{\rm RCB}R_B'^{1/(\gamma-1)}r^{\frac{2\gamma-3}{\gamma-1}}\frac{dr}{r} \tag{B5}$$

If $\gamma < 3/2$ then the main contribution to the energy is at the bottom of the atmosphere, i.e. the core. This is the case for a diatomic ideal gas ($\gamma = 1.4$) or a solar mixture of hydrogen and helium ($\gamma \approx 1.43$). However a monatomic gas has $\gamma = 5/3 > 3/2$. In this case, the atmosphere's energy is no longer concentrated near the bottom, but will be concentrated near the top of the convective zone.

A likely structure is an atmosphere that is dissociated near the base, but becomes molecular near the top of the convective zone. In this case the atmosphere's energy budget would be concentrated near the atomic to molecular transition.

The energy required to dissociate a hydrogen molecule, $I = 4.467$ eV can be significant to the overall energy budget. Since

$$\frac{I}{\nabla_{\rm ad}GM_{\rm c}(2m_{\rm H})/r} \approx 3\left(\frac{M_{\rm c}}{10M_\oplus}\right)^{-2/3}\frac{r}{R_{\rm c}} \tag{B6}$$

we see that this energy is always relevant.

We can use the Saha equation to determine where dissociation is significant,

$$\frac{n_{\rm H}^2}{n_{\rm H_2}} = \left(\frac{\pi m_{\rm H}kT}{h}\right)^{3/2}e^{-I/(kT)} \tag{B7}$$

We introduce a reaction coordinate δ so that $n_{\rm H} = 2\delta n_o$ and $n_{\rm H_2} = (1-\delta)n_o$ with $n_o = \rho X/(2m_{\rm H})$ the number density when all hydrogen is molecular. We express equilibrium as

$$\frac{\delta^2}{1-\delta} = f_\mu\frac{P_{\rm diss}(T)}{P} \tag{B8}$$

with the characteristic pressure below which dissociation occurs is

$$P_{\rm diss} = \frac{(kT)^{5/2}}{4}\left(\frac{\pi m_{\rm H}}{h^2}\right)^{3/2}e^{-I/(kT)} \tag{B9}$$

and the order unity factor

$$f_\mu = 2\delta + (1-\delta) + Y/2 + Z/\mu_Z \tag{B10}$$

accounts for variations in the mean molecular weight with dissociation. (Take $\mu_Z = 31/2$, but not too significant.)

Thus dissociation occurs where $P \lesssim P_{\rm diss}(T)$. At disk temperatures (say 150 K) the dissociation pressure is negligibly small ($\sim 10^{-141}$ dyne cm^{-2}) and no dissociation occurs. However at core temperatures the dissociation pressure is quite large especially for massive cores. Dissociation is guaranteed.